Title

Isolation and Biosynthesis of Hyellamide, a Glycosylated N-Acyltyrosine Derivative, from the Cyanobacterium Hyella patelloides LEGE 07179.

Journal

Journal of natural products, 88(3)

Authors

Brito, Ângela

Martins, Teresa

Freitas, Sara

et al.

Publication Date

2025-03-28

DOI

10.1021/acs.jnatprod.4c00968

Peer reviewed

JOURNAL OF NATURAL PRODUCTS

pubs.acs.org/jnp

Note

Isolation and Biosynthesis of Hyellamide, a Glycosylated N-Acyltyrosine Derivative, from the Cyanobacterium *Hyella patelloides* LEGE 07179

Ângela Brito, Teresa Martins, Sara Freitas, Raquel Castelo Branco, Adriana Rego, Vitor M. Vasconcelos, William H. Gerwick, Paula Tamagnini, and Pedro N. Leão*

Cite This: *J. Nat. Prod.* 2025, 88, 850−856

Read Online

ACCESS | Metrics & More | Article Recommendations | Supporting Information

ABSTRACT: Recent analyses of genome data indicate that members of the cyanobacterial order Pleurocapsales show tremendous potential for natural product discovery. However, only a few compounds have been reported from this order. Here, we report the isolation of hyellamide (**1**), a glycosylated N-acyl tyrosine-derived eneamide, from the pleurocapsalean cyanobacterium *Hyella patelloides* LEGE 07179. The putative biosynthetic gene cluster for **1** was identified in the genome of the producing organism and a biosynthetic proposal is presented. This work sheds light on the chemistry of the Pleurocapsales and expands the chemical repertoire of cyanobacterial natural products to include N-acyl tyrosine-derived molecules.

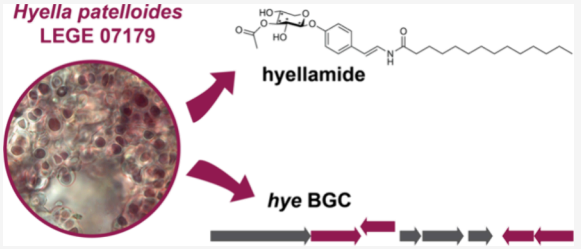

The phylum Cyanobacteria is well-known for its rich secondary metabolism. Chemical exploration of these organisms has led to the discovery of potent toxins or cytotoxic scaffolds that made their way into several drugs or drug candidates.[1,2] Over the past 50 years, hundreds of natural products have been reported from filamentous cyanobacteria of the orders Oscillatoriales and Nostocales, which have been the main targets of discovery efforts.[1] However, recent genome surveys have indicated that members of the order Pleurocapsales are among the biosynthetically richest cyanobacteria,[3−5] despite being underrepresented in genome data.[2−5] In fact, as of March 2024, there are only four reference genomes for this order in the NCBI, among 51 total pleurocapsalean genome entries, most of which correspond to metagenome-assembled genomes (MAGs).

In spite of the rich potential of members of the Pleurocapsales for production of secondary metabolites, the order remains underexplored for new chemistry. Hyellazole and its chlorinated derivative chlorohyellazole[6] are the only reported pleurocapsalean secondary metabolites (Natural Products Atlas,[7] accessed March 27, 2024), although the UV-protective pigment scytonemin has been linked to members of this order.[8] Unusual biosynthetic chemistry leading to beta-amino acids has been investigated in *Pleurocapsa* sp. strains,[9] but the natural products encoded by such unusual pathways have not been determined.

We have recently reported[3] genomic data for the single representative of the *Hyella patelloides* species, *H. patelloides* LEGE 07179, a member of the Pleurocapsales. Its genome contained 21 biosynthetic gene clusters (BGCs) of different biosynthetic classes, which sparked our interest for exploring its natural products diversity. In this study, following large-scale culturing of this slow-growing strain, we isolated and purified from its biomass a new glycosylated N-acyl tyrosine-derived eneamide, which we named hyellamide (**1**). By mining the genome of *H. patelloides* LEGE 07179, we have pinpointed the putative BGC encoding **1** and put forward a proposal for its biosynthesis.

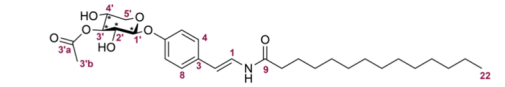

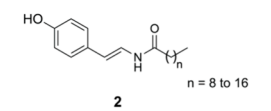

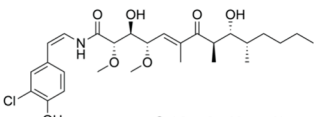

BIOACTIVITY-GUIDED COMPOUND PURIFICATION

Motivated by the diversity of BGCs found in the genome of *H. patelloides* LEGE 07179,[3] we sought to explore this strain for its bioactive chemical constituents. Large-scale cultivation (300 L) of the strain yielded 135 g (d.w.) of biomass, which was

Received: August 22, 2024
Revised: February 10, 2025
Accepted: February 12, 2025
Published: February 26, 2025

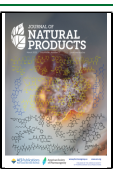

https://doi.org/10.1021/acs.jnatprod.4c00968
J. Nat. Prod. 2025, 88, 850−856

Table 1. ^{1}H and ^{13}C NMR Spectroscopic Data of Hyellamide (1) in $CDCl_3$[ab]

unit	no.	δ_C, type	δ_H (J in Hz)	HMBC	COSY
4-[(*E*)-2-aminovinyl]phenol	1	122.1, CH	7.43, dd (14.6, 10.8)	2, 3, 4/8, 9	2, NH-1
	NH-1	-	7.11, d (11.8)	1, 2, 4/8, 9	1
	2	111.8, CH	6.03, d (14.7)	1, 4/8, 3	1
	3	131.2, C	-	-	-
	4	126.8, CH	7.25, d (8.9)	2, 5/7, 6, 8	5, 7
	5	117.3, CH	6.96, d (8.7)	3, 6, 7	4, 8
	6	155.6, C	-	-	-
	7	117.3, CH	6.96, d (8.7)	3, 5, 6	4, 8
	8	126.8, CH	7.25, d (8.9)	2, 4, 5/7, 6	5
	9	170.6, C	-	-	-
Tetradecanoic acid	10	37.0, CH_2	2.27, t (7.6)	9, 11	11
	11	25.6, CH_2	1.68, m	9, 10, 12	10, 12
	12−19	29.8−29.4, CH_2	1.34−1.25, m		
	20	32.1, CH_2	1.34−1.25, m		
	21	22.8, CH_2	1.28, m	20, 22	22
	22	14.3, CH_3	0.88, t (7.0)	20, 21	21
β-D-4-*O*-acetyl-xylopyranose	1′	100.8, CH	5.04, d (6.2)	2′, 3′, 5′, 6	2′
	2′	70.5, CH	3.83, dd (6.1, 7.9)	1′, 3′, 4′	1′, 3′
	3′	76.6, CH	4.91, t (7.8)	1′,2′, 3′a, 4′, 5′	2′, 4′
	3′a	172.4, C	-	-	-
	3′b	21.2, CH_3	2.20, s	3′, 3′a	-
	4′	68.6, CH	3.86, dd (7.8, 4.6, 8.2)	2′, 3′, 5′	3′, 5′a, 5′b
	5′a	64.9, CH2	4.14, dd (4.6, 11.9)	4′, 3′, 1′	4′, 5′b
	5′b		3.48, dd (8.2, 11.9)	4′, 3′, 1′	4′, 5′a

[a]Data recorded at 600 MHz (^{1}H) and 150 MHz (^{13}C). [b]Data obtained for partially purified fraction F9_3, containing **1** and a PUFA. For comparison of the ^{1}H NMR spectra of this fraction and of pure **1**, see Figure S2.

subjected to CH_2Cl_2:MeOH (2:1) extraction. The resulting extract (15.0 g) was fractionated by normal-phase vacuum liquid chromatography (VLC) yielding 10 fractions of increasing polarity. These VLC fractions were tested for antimicrobial activity using the disk diffusion method. Considerable antimicrobial activity against the Gram-positive *B. subtilis* and *S. aureus* was observed in three midpolarity fractions (D to F). These fractions were combined and further fractionated by reversed-phase flash chromatography. Three of the resulting fractions exhibited antimicrobial activity and were pooled and refractionated using semipreparative HPLC. This procedure led to a single subfraction showing strong antimicrobial activity (as evaluated by inhibition in disk assays), which was selected for further fractionations through a series of analytical-scale HPLC separations. This eventually yielded partially purified fraction F9_3 (1.4 mg), containing hyellamide (**1**) and a compound with NMR signals consistent with a polyunsaturated fatty acid (PUFA), to which we attributed the antimicrobial activity (see below and Figure S1). 1D and 2D NMR data were acquired for this fraction, as it was not clear initially whether it corresponded to a single pure compound. Further analysis of this data set revealed that the fraction was a binary mixture but still allowed for structure elucidation of compound **1**. Subsequent analytical-scale HPLC separation of fraction F9_3 yielded a small amount of compound **1** (0.4 mg), which was used for recording physical characterization data and bioactivity testing (see below and Figure S1).

STRUCTURE ELUCIDATION OF 1

HRESIMS analysis of **1** indicated a protonated molecule $[M + H]^+$ at m/z 520.3268, consistent with a molecular formula of $C_{29}H_{46}NO_7$ and eight degrees of unsaturation. Searches in the Natural Products Atlas[7] returned no hits for this accurate mass from cyanobacteria. Inspection of the ^{1}H NMR data ($CDCl_3$) for **1** (Figures S2 and S3) revealed the presence of six aromatic or olefinic protons (δ_H 7.5−6.0), six heteroatom-associated deshielded protons (δ_H 5.1−3.4), a methyl singlet (δ_H 2.20), two aliphatic methylenes (δ_H 2.27 and 1.68), a large methylene envelope (δ_H 1.34−1.25) and a methyl group triplet resonating at δ_H 0.88. The ^{13}C APT NMR data for **1** in the same solvent (Figure S4) indicated the presence of two ester or amide carbonyls (δ_C 172.4, 170.6), four discrete signals for six aromatic or olefinic carbons with attached methine protons (δ_C 126.8.-111.8), two nonprotonated aromatic carbons (δ_C 155.6, 131.2), one diagnostic anomeric carbon (δ_C 100.4), three oxymethines (δ_C 77.6−68.6), an oxygenated methylene (δ_C 64.9), a slightly deshielded methylene resonance at δ_C 37.0, and a large number of methylene signals ranging from δ_C 32.1−25.6, consistent with the methylene envelope observed in the ^{1}H NMR spectrum. One additional methylene group (δ_C 21.2) and two methyl groups (δ_C 22.8, 14.3) were also identifiable in the data.

We resorted to combined analysis of 1D (^{1}H, ^{13}C APT) and 2D (HSQC, HMBC, COSY) NMR experiments in $CDCl_3$ to fully elucidate the planar structure of **1** (Table 1, Figures S3−S7, Figure 1A). These were carried out using purified fraction F9_3, containing **1** and a PUFA contaminant, as detailed previously. A spin system from H_2-22 to H_2-20 was clearly established through COSY correlations, which was itself correlated to the methylene envelope (Table 1, Figure 1). An additional spin system from H_2-10 to H_2-12, established from COSY correlations, also linked to the methylene envelope. The H_2-10 methylene was HMBC correlated to the C-9 carbonyl (δ_C 170.6), thereby establishing an aliphatic acyl chain. Given the presence of the PUFA impurity in the

https://doi.org/10.1021/acs.jnatprod.4c00968
J. Nat. Prod. 2025, 88, 850−856

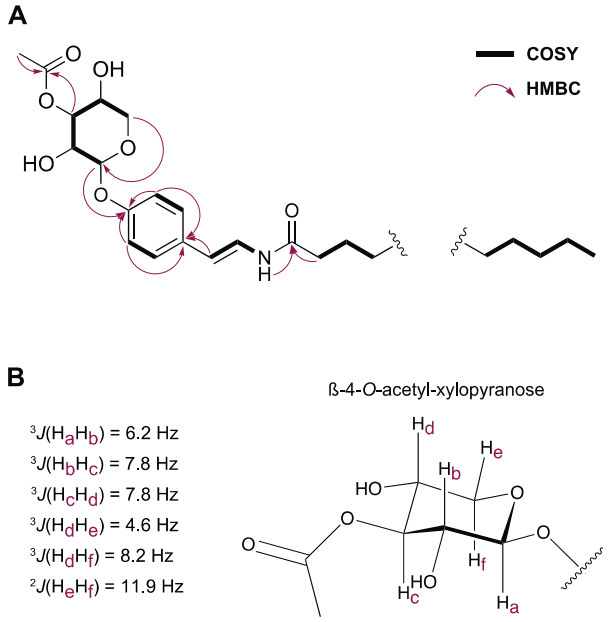

Figure 1. Structure elucidation of hyellamide (**1**). (A) Key HMBC and COSY correlations obtained from NMR analysis of **1**. (B) Coupling constant analysis establishing the relative configuration of the acetylated xylose residue in **1**.

sample, the size of this chain could not be determined through integration of the methylene envelope. A *para*-substituted phenolic aromatic system was also readily inferred from the combined data analysis (Table 1, Figure 1B). In this aromatic system, H-4/H-8 showed HMBC correlations to the olefinic carbon C-2, which itself was part of a COSY-established spin system comprising C-2, C-1 and NH-1 (δ_H 7.11). This resulted in the establishment of a nitrogen-bound vinylphenol moiety.

An additional spin system could be established from COSY correlations of an anomeric proton (H-1′), three oxymethine signals (H-2′/3′/4′) and two deshielded methylene protons (H_2-5′). The latter were HMBC correlated to the anomeric carbon C-1′, establishing a pyranosyl moiety. This was found to be decorated with an acetyl unit at position 3′ based on HMBC correlations from H-3′ and H_3-3′b to the carbonyl C-3′a (δ_C 172.4). This acetylated sugar residue was found to be a substituent on the phenol group, based on an HMBC correlation from the anomeric proton to the aromatic carbon C-6. Finally, HMBC correlations from the NH-1 proton at δ_H 7.11 and H-1 to the C-9 carbonyl (δ_C 170.6) indicated that an amide bond connected the sugar-substituted 4-vinylphenol moiety to the aliphatic chain, which established the planar structure of **1**. Coupling constant analysis (Figure 1C) indicated that the modified sugar moiety was xylose, connected through a β-linkage. Supplementation of D- or L-xylose to cultures of *H. patelloides* LEGE 07179 did not lead to differential production of **1** (Figure S8). Because the D-form is the natural form of xylose and L-xylose is extremely rare in nature,[10] the 4-*O*-acetyl-xylopyranose residue in **1** is proposed here to be in a D-configuration, but this proposal requires future validation. The configuration of the olefin was found to be *trans*, as per the large coupling constant (14.7 Hz). Analysis

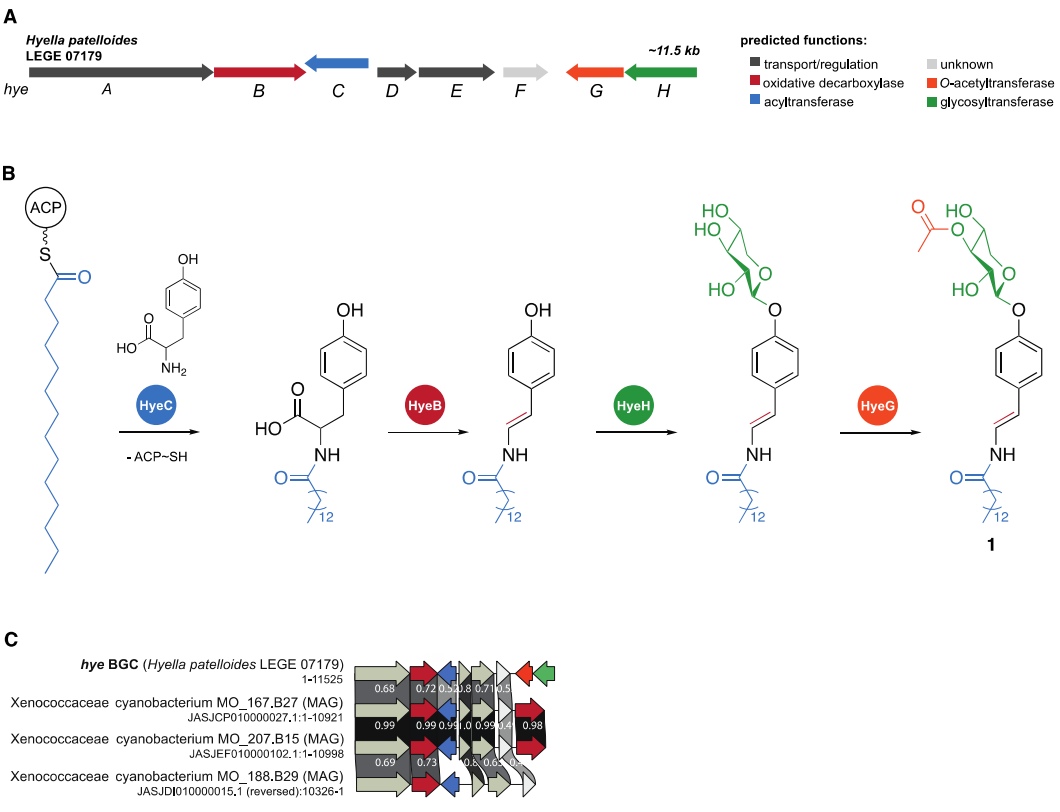

Figure 2. Proposed biosynthesis of hyellamide (**1**). (A) Organization of the *hye* BGC of *Hyella patelloides* LEGE 07179, proposed to be involved in the biosynthesis of **1**. (B) Proposed biosynthesis steps leading to the production of **1**. (C) Additional *hye*-like BGCs found in publicly available cyanobacterial genomes/MAGs (minimum of 30% of similarity and 50% of query coverage), homologous genes in different clusters are connected through shaded regions, darker shaded indicate higher identity.

https://doi.org/10.1021/acs.jnatprod.4c00968
J. Nat. Prod. 2025, 88, 850−856

of the fragmentation data for **1** (HRESIMS/MS) supported the proposed structure (Figure S9).

Compound **1** represents a new natural product scaffold combination, namely of an *N*-acylated tyrosine eneamide with an (acetylated) sugar moiety. Related compounds include nonglycosylated tyrosine-derived eneamides (**2**) reported by Brady and co-workers from heterologous expression of soil-derived eDNA,[11] which contain fatty acyl chains, and the chondrochlorens (e.g., **3**),[12] in which the *N*-acyl chains are branched and decorated, as typical of polyketides.

The function for (nonglycosylated) N-acyl amino acid metabolites in bacteria remains largely unknown, despite reports of antibacterial activity and biosurfactant properties.[13] When pure **1** was tested in the antibacterial activity assay against *Bacillus subtilis* ATCC 16633 that had been used to guide the isolation, no inhibition halo was observed (Figure S1), suggesting that the activity observed and followed during the isolation process was likely due to the coeluting PUFA, as mentioned above. C13:0 to C16:0 *N*-acylated tyrosines were found to be active against *B. subtilis* by Brady and Clardy.[14] This implies that the substantial modifications to the tyrosyl moiety in **1** (C14:0 acylated), i.e. decarboxylation and/or glycosylation, negatively impact the antibacterial activity of the scaffold.

IDENTIFICATION OF THE HYELLAMIDE BIOSYNTHETIC GENE CLUSTER (*hye*)

We sought to identify a plausible candidate BGC for the biosynthesis of **1** through genome analysis of *H. patelloides* LEGE 07179. To this end, we considered that the gene encoding the biosynthetic step leading to the eneamide moiety in **1** would be the least likely to contain multiple homologues in the genome. In the biosynthesis of soil eDNA-derived enamides (**2**), this step has been proposed to result from decarboxylative oxidation of the *N*-acylated tyrosine moiety by the flavin-dependent oxidase FeeG.[11] The BGC associated with the production of the chondrochlorens encodes an enzyme with homology to FeeG (CndG), which was shown to catalyze a similar reaction.[15] tBlastn searches against the *H. patelloides* LEGE 07179 genome (GenBank accession GCA_900659865) using FeeG as query led to a single hit (gene product herein named HyeB, accession WP_144872799; 32% identity, 52% similarity), close to a contig edge. To obtain larger flanking regions, we resequenced the genome of *H. patelloides* LEGE 07179 using illumina technology, and this time the gene encoding the FeeG homologue contained much larger flanking regions. Analysis of the genomic context of this gene revealed functions compatible with the biosynthesis of **1**, including an acyltransferase and a glycosyltransferase (Figure 2a, Table S1). We thus propose that this locus corresponds to the hyellamide BGC (*hye*) (Figure 2a, Table S1). Based on the architecture of the *hye* BGC and previous biochemical knowledge associated with homologues of the *hye*-encoded enzymes, we propose (Figure 2b) that the biosynthesis of **1** begins with the myristoylation of tyrosine by the acyltransferase HyeC. This enzyme is annotated as a putative fatty acyl transferase from the SGNH/GDSL hydrolase protein family. We suggest that the acyl moiety is provided by a myristoyl-ACP thioester, since ACP-bound fatty acids seem to be the major contributors of medium-to-long chain acyl moieties for secondary metabolism in cyanobacteria.[16] Unlike in the biosynthesis of **2**,[11] no dedicated ACP or fatty acid-activating enzyme was found in the vicinity of the *hye* locus and thus these intermediates could be retrieved from primary metabolism (fatty acid biosynthesis). Tyrosine could then undergo oxidative decarboxylation by the FeeG/CndG homologue HyeB, as observed in the biosynthesis of **2** and **3**, respectively.[11,15] The glycosyltransferase HyeH could then decorate the phenol ring, likely using xylosyl-UDP as a substrate. Finally, 4-*O*-acetylation is proposed to be performed by the putative acetyltransferase HyeG. The sequence of this latter protein is annotated as a DapH/DapD/GlmU-related protein, associated with the trimeric LpxA-like superfamily (InterPro IPR011004), which encompasses several acyltransferases, including sugar acetyltransferases.

Searches for the *hye* BGC in publicly available cyanobacterial genomes/ MAGs (nr database) indicated that related BGCs, containing the key HyeB decarboxylase (but lacking homologues for HyeH and HyeG), are found in MAGs attributed to Xenococcaceae cyanobacteria, a pleurocapsalean sister family of the Hyellaceae (where the *Hyella* genus is placed) (Figure 2c). Some of these BGCs encode an additional HyeB homologue. An extended search (nr database) revealed HyeB homologues to be distributed across distinct bacterial phyla (Figure S10), although a similar BGC architecture and genomic context is only maintained in the MAGs attributed to Xenococcaceae cyanobacteria.

CONCLUSIONS

Chemical exploration of *Hyella patelloides* LEGE 07179 led to the discovery of an *N*-acylated tyrosine-like molecule, hyellamide (**1**), which differs from previously reported related compounds, namely the soil-derived *N*-acylated tyrosine-derived eneamides such as compound **2**, due to the decoration of its phenol ring with a sugar unit. Compound **1** can thus be considered yet another type of cyanobacterial glycolipid. This is only the second class of secondary metabolites reported from the Pleurocapsales order, which have been shown bioinformatically to be the richest among cyanobacteria in terms of BGCs per genome.[4,5] It is also the first report of a compound of this class or of a related compound from cyanobacteria. The proposed biosynthesis of **1** employs the same eneamide-generating decarboxylative oxidation step that occurs during the biosynthesis of *N*-acylated tyrosine-derived eneamides such as **2** and **3**.[11,15] However, the BGC that we associate with compound **1** contains elements diverging from such pathways, namely the *N*-acylating enzyme and, obviously, the enzymes involved in the incorporation and modification of the sugar residue. Curiously, this was the only BGC of this type found in publicly available databases; a few similar BGCs were found in other cyanobacteria, but without the genes encoding glycosylation and *O*-acetylation of the sugar moiety. This study reinforces that the understudied Pleurocapsales order is a promising taxon to discover novel natural product scaffolds.

EXPERIMENTAL SECTION

General Experimental Procedures. Optical rotation was recorded in MeOH using a JASCO P-2000 polarimeter with SpectraManager 2.14.02 software. A UV absorption spectrum was measured in MeOH on a UV-1600PC spectrometer (VWR) controlled by MWAVE 1.0.20 software. An infrared spectrum was acquired on a Nicolet iS5 FTIR spectrometer (Thermo Scientific) with OMNIC 9.8.372 software. 1D and 2D NMR data were obtained on a Bruker Avance III, 600 MHz, equipped with a 5 mm cryoprobe and controlled by Topspin 3.6.2, from the Materials Centre of the

https://doi.org/10.1021/acs.jnatprod.4c00968
J. Nat. Prod. 2025, 88, 850−856

University of Porto (CEMUP). NMR spectra were acquired in deuterated chloroform ($CDCl_3$) and chemical shifts (δ) are expressed in parts per million (ppm) relative to $CDCl_3$ (δ_C 77.16, δ_H 7.26). NMR data were analyzed in MNova 14.0.0 (MestreLab Research). LC-HRESIMS and LC-HRESIMS/MS analyzes were performed on an Ultimate 3000 UHPLC (Thermo Fisher Scientific) system composed of an LPG-3400SD pump, WPS-3000SL autosampler and VWD-3100 UV/vis detector coupled to a Q Exactive Focus Hybrid Quadrupole-Orbitrap mass spectrometer controlled by Q Exactive Focus Tune 2.9 and Xcalibur 4.1 software (Thermo Fisher Scientific). LC-HRESIMS data were obtained in Full Scan mode with a scan range of m/z 200−2000, capillary voltage set to -3.8kV, capillary temperature to 300 °C and sheath gas flow rate to 35 units. HPLC separations were performed with an Alliance e2695 associated with a Photodiode array (PDA) 1998 detector (Waters) and the chromatography was monitored with fixed wavelengths of 254 nm, 280 and 400 nm, and a max plot (PDA) from 210 to 400 nm. All solvents used were ACS grade, except for HPLC and LC-MS solvents (HPLC and LC-MS grades, respectively).

Cyanobacterial Strain and Culture Conditions. The cyanobacterium *Hyella patelloides* LEGE 07179 was previously isolated from the Portuguese coast and is deposited at the LEGE Culture Collection (CIIMAR, Matosinhos, Portugal). This strain was maintained in MN medium supplemented with 10 μg mL^{-1} of B_{12} vitamin, at 25 °C, under 16 h light (~10 μmol photons m^{-2} s^{-1})/8 h dark regimen. The large-scale cultivation was carried out in 75 L low density polyethylene sleeves for a total of 150 L and using 10 and 20 L polycarbonate carboys (Thermo Fisher Scientific) for a total of 150 L as well. Biomass was harvested after 3 months of growth and freeze-dried until further used. Substrate supplementation experiments with D- and L-xylose were performed in order to ascertain if production of **1** increases when these exogenous substrates are added to the cultures. To this end, triplicate cultures of *H. patelloides* (~0.1 OD 750 nm) were grown under the conditions mentioned above, but containing 1 mM L- or D-xylose. Following a 7-day growth period, the cultures were extracted as detailed below for large-scale extraction and the resulting extracts submitted for LC-HRESIMS analysis.

Extraction and Isolation of Hyellamide. To produce the crude organic extract, 135 g of freeze-dried biomass of *Hyella patelloides* LEGE 07179 was repeatedly extracted with 2:1 CH_2Cl_2:MeOH (v/v) at room temperature and twice at 30 °C. The resulting crude extract (15.0 g) was fractioned by vacuum liquid chromatography (VLC), using silica gel 60 (0.015−0.040 mm, Merck). The extract was first solubilized with CH_2Cl_2 and MeOH and adsorbed to silica particles through solvent evaporation. Subsequently, the extract-adsorbed silica was loaded onto a dry-packed column. Initially, a mixture of 10% EtOAc/90% hexanes was employed to start the separation, followed by an increasing polarity gradient to 100% EtOAc and then to 100% MeOH, yielding ten fractions (A - J). Fractions with antimicrobial activity (D-F, eluting from 3:2 EtOAc:hexanes to 1:9 MeOH:hexanes, v/v) were pooled and further fractionated by reversed-phase flash chromatography (Pure C-850 FlashPrep, BÜCHI) using a Flash Cartridge C18, 120 g (40 to 63 μm, 60 Å, SiliCycle), at 45 mL min^{-1} flow rate. The dry loading was performed as described above and a solvent gradient was used starting from 30% MeOH/70% H_2O to reach 100% MeOH over 40 min and held at 100% MeOH for 15 min, and then 100% EtOAc for 5 min, yielding 22 fractions. Three fractions exhibiting antimicrobial activity were pooled and subjected to semipreparative HPLC using a Synergi Fusion-RP column (4 μm, 250 × 10 mm, 80 Å; Phenomenex). The elution was performed at a flow rate of 3 mL min^{-1}, starting with an isocratic step 50% MeOH/50% H_2O for 5 min followed by a gradient to reach 80% 2-propanol/15% MeOH/5% H_2O over 25 min, and held for 5 min before returning to the initial conditions. This procedure afforded 15 subfractions. One of the fractions (Fraction 9) was selected for HPLC separation using an ACE Excel 3 C18-AR column (3 μm, 75 × 4.6 mm, 100 ***; Avantor) at 0.6 mL min^{-1} flow rate. A gradient elution program started with 50% MeOH/50% H_2O to reach 50% MeOH/25% 2-propanol/25% H_2O for 30 min and held for 6 min before returning to the initial conditions. This procedure afforded four subfractions. ^{1}H NMR analysis indicated that subfraction F9−3 contained a mixture of a polyunsaturated fatty acid (PUFA) and of an unknown compound. 2D NMR data were acquired for this fraction and allowed for the structure elucidation of **1**. However, to obtain physical and biological characterization data for **1**, subfraction F9−3 was subjected to an additional purification step in the same system but with a gradient starting at 40% MeOH/60% H_2O to reach 70% MeOH/20% 2-propanol/10% H_2O for 30 min and returning to the initial conditions. Subfraction F9−3.2 underwent an additional purification step in the same system, employing a gradient elution starting at 60% CH_3CN/40% H_2O to reach 100% CH_3CN over 16 min and held for 8 min before returning to the initial conditions, affording four subfractions. Subfraction F9−3.2.2 (compound **1**, 0.4 mg) was spectroscopically pure (>95%, ^{1}H NMR).

Hyellamide (1). Amorphous, white power; $[\alpha]^{23}_D$ −27.4 (c 0.067, MeOH); UV (MeOH) λ_{max} (log ε) 221 (3.54), 275 (3.57), 287 (3.57) nm (see Figure S11); IR ν_{max} 3296, 2919, 2850, 2285, 1717, 1635, 1575, 1559, 1540, 1506, 1471 cm^{-1} (see Figure S12); 1D and 2D NMR data (see Table 1 and Figures S2−S7); LC-HRESIMS m/z 520. 3268 $[M + H]^+$ (calcd for $C_{29}H_{46}NO_7$, 520.3269). LC-HRESIMS/MS data (see Figure S9).

LC-HRESIMS and LC-HRESIMS/MS Analyses. For LC-HRESIMS and LC-HRESIMS/MS analysis, fractions were prepared at 0.5 mg mL^{-1} in LC-MS grade MeOH and then filtered through a 0.2 μm syringe regenerated cellulose filter. Separation was performed in an ACE Ultracore 2.5 SuperC18 column (75 × 2.1 mm) with a flow rate of 0.350 mL min^{-1} and using the following gradient: 10% CH_3CN/90% H_2O to reach 100% CH_3CN over 8 min and then 30% CH_3CN/70% 2-propanol for 6 min and held for 1 min before returning to the initial conditions. The column oven was set to 40 °C, and UV monitoring was carried out at 254.0 nm. MS/MS parameters for the LC-HRESIMS/MS analysis were: resolution of 35000, with a 1 m/z isolation window, a loop count of 3, AGC target of 5 × 10^4 and collision energy of 35 eV.

Genome and Bioinformatic Analyses. The amino acid sequence of FeeG was used as query in a blastP search against the previously reported genome of *Hyella patelloides* LEGE 07179.[3] A single hit was found (WP_144872799), encoded close to the contig edge in the corresponding nucleotide sequence. We thus resequenced the genome of this organism to attempt to obtain a larger genomic context for the FeeG homologue. gDNA was isolated from a fresh pellet of this strain using the PureLink Genomic DNA Mini Kit (Life Technologies) as per the manufacturers' instruction. The gDNA was sequenced by MicrobesNG, UK using Illumina technology (2 × 250 bp paired-end reads). Quality-filtered raw reads were assembled into contigs by the sequencing services provider. The gene encoding the FeeG homologue (HyeB) was located in a longer (~30 kb) contig (NCBI: PQ095878), flanked by roughly 13 kb upstream and 15 kb downstream, thus enabling the analysis of its genomic context and annotation of the *hye* locus, which was carried out using blastP searches against the nr database (Table S1). To better understand the diversity of *hye*-like BGCs and of HyeB-encoding genes and their genomic context in other organisms, a comparative analysis was performed using all publicly available cyanobacteria genomes and MAGs and also against the nr database in NCBI. A total of 5355 cyanobacterial genomes were downloaded from NCBI using NCBI Data sets command line (CLI) download tool (assessed on 8 March 2024). GenBank files were used to create a local database for identification and visualization of homologous gene clusters using cblaster.[17] The *hye* BGC was used as a query, considering a minimum of 30% similarity and 50% of query coverage. GenBank files of target gene clusters were extracted using "cblaster extract_clusters" and clinker[18] was used for gene cluster comparison visualization. A cblaster analysis using the *hyeB* gene as query (minimum 30% of similarity and 50% of query cover) against the nr database was computed using the CAGECAT Web server.[19] The top 40 hits were extracted and a CORASON[20] analysis was performed to identify the genomic context in which HyeB homologues can be found.

Antimicrobial Assays. The antimicrobial assays used the agar disk diffusion method as previously described.[21] Solutions of 1 mg

https://doi.org/10.1021/acs.jnatprod.4c00968
J. Nat. Prod. 2025, 88, 850−856

mL^{-1} of the different fractions (prepared in DMSO) were tested against the Gram positive bacteria *Bacillus subtilis* ATCC 6633 and *Staphylococcus aureus* ATCC 29213, the Gram-negative *Escherichia coli* ATCC 25922 and *Salmonella typhimurium* ATCC 25241 and the fungus *Candida albicans* ATCC 1023. Fifteen microliters (15 μL) of the test solutions were added to each disk.

■ ASSOCIATED CONTENT

Data Availability Statement

The NMR data for **1** has been deposited in the Natural Products Magnetic Resonance Database (NP-MRD; www.np-mrd.org) and can be found under NP0333068. LC-HRESIMS/MS data for **1** was submitted to the GNPS Library (bronze) under accession CCMSLIB00012194749. The DNA sequence corresponding to the contig harboring the proposed *hye* BGC was uploaded to the NCBI under accession PQ095878.

Supporting Information

The Supporting Information is available free of charge at https://pubs.acs.org/doi/10.1021/acs.jnatprod.4c00968.

Antimicrobial assay data, NMR, HRESIMS/MS, UV and FT-IR spectra, xylose supplementation experiment data, CORASON phylogenetic reconstruction, annotation of the *hye* BGC (PDF)

■ AUTHOR INFORMATION

Corresponding Author

Pedro N. Leão − *CIIMAR - Interdisciplinary Centre of Marine and Environmental Research, University of Porto, 4450-208 Matosinhos, Portugal;* orcid.org/0000-0001-5064-9164; Phone: +351223401800; Email: pleao@ciimar.up.pt

Authors

Ângela Brito − *Instituto de Investigação e Inovação em Saúde, Universidade do Porto, 4200-135 Porto, Portugal; IBMC - Instituto de Biologia Molecular e Celular, Universidade do Porto, 4200-135 Porto, Portugal*

Teresa Martins − *CIIMAR - Interdisciplinary Centre of Marine and Environmental Research, University of Porto, 4450-208 Matosinhos, Portugal; ICBAS - School of Medicine and Biomedical Sciences, University of Porto, 4050-313 Porto, Portugal*

Sara Freitas − *CIIMAR - Interdisciplinary Centre of Marine and Environmental Research, University of Porto, 4450-208 Matosinhos, Portugal; Faculdade de Ciências, Departamento de Biologia, Universidade do Porto, 4169-00 Porto, Portugal*

Raquel Castelo Branco − *CIIMAR - Interdisciplinary Centre of Marine and Environmental Research, University of Porto, 4450-208 Matosinhos, Portugal; Faculdade de Ciências, Departamento de Biologia, Universidade do Porto, 4169-00 Porto, Portugal*

Adriana Rego − *CIIMAR - Interdisciplinary Centre of Marine and Environmental Research, University of Porto, 4450-208 Matosinhos, Portugal*

Vitor M. Vasconcelos − *CIIMAR - Interdisciplinary Centre of Marine and Environmental Research, University of Porto, 4450-208 Matosinhos, Portugal; Faculdade de Ciências, Departamento de Biologia, Universidade do Porto, 4169-00 Porto, Portugal*

William H. Gerwick − *Center for Marine Biotechnology and Biomedicine, Scripps Institution of Oceanography, University of California San Diego, La Jolla, California 92093, United States; Skaggs School of Pharmacy and Pharmaceutical Sciences, University of California San Diego, La Jolla, California 92093, United States;* orcid.org/0000-0003-1403-4458

Paula Tamagnini − *Instituto de Investigação e Inovação em Saúde, Universidade do Porto, 4200-135 Porto, Portugal; IBMC - Instituto de Biologia Molecular e Celular, Universidade do Porto, 4200-135 Porto, Portugal; Faculdade de Ciências, Departamento de Biologia, Universidade do Porto, 4169-00 Porto, Portugal;* orcid.org/0000-0003-4396-2122

Complete contact information is available at: https://pubs.acs.org/10.1021/acs.jnatprod.4c00968

Notes

The authors declare no competing financial interest.

■ ACKNOWLEDGMENTS

This work was funded by national funds through FCT (Fundação para a Ciência e a Tecnologia), within the scope of strategic funding grants UIDB/04423/2020, UIDP/04423/2020, UIDB/04293/2020 and UIDP/04293/2020, as well as postdoctoral research grant SFRH/BPD/115571/2016 (AB). The study was funded also through the European Union's Horizon 2020 Research and Innovation Programme (GA no. 952374) and European Research Council (GA 759840).

■ REFERENCES

(1) Demay, J.; Bernard, C.; Reinhardt, A.; Marie, B. *Marine Drugs* **2019**, *17* (6), 320.

(2) Baunach, M.; Guljamow, A.; Miguel-Gordo, M.; Dittmann, E. *Nat. Prod. Rep.* **2024**, *41* (3), 347−369.

(3) Brito, Â.; Vieira, J.; Vieira, C. P.; Zhu, T.; Leão, P. N.; Ramos, V.; Lu, X.; Vasconcelos, V. M.; Gugger, M.; Tamagnini, P. *Front. Microbiol.* **2020**, *11*, 1527.

(4) Jung, P.; D'Agostino, P. M.; Brust, K.; Büdel, B.; Lakatos, M. *Life* **2021**, *11* (9), 916.

(5) Gavriilidou, A.; Kautsar, S. A.; Zaburannyi, N.; Krug, D.; Müller, R.; Medema, M. H.; Ziemert, N. *Nat. Microbiol* **2022**, *7* (5), 726−735.

(6) Cardellina, J. H.; Kirkup, M. P.; Moore, R. E.; Mynderse, J. S.; Seff, K.; Simmons, C. J. *Tetrahedron Lett.* **1979**, *20* (51), 4915−4916.

(7) van Santen, J. A.; Jacob, G.; Singh, A. L.; Aniebok, V.; Balunas, M. J.; Bunsko, D.; Neto, F. C.; Castaño-Espriu, L.; Chang, C.; Clark, T. N.; Cleary Little, J. L.; Delgadillo, D. A.; Dorrestein, P. C.; Duncan, K. R.; Egan, J. M.; Galey, M. M.; Haeckl, F. P. J.; Hua, A.; Hughes, A. H.; Iskakova, D.; Khadilkar, A.; Lee, J.-H.; Lee, S.; LeGrow, N.; Liu, D. Y.; Macho, J. M.; McCaughey, C. S.; Medema, M. H.; Neupane, R. P.; O'Donnell, T. J.; Paula, J. S.; Sanchez, L. M.; Shaikh, A. F.; Soldatou, S.; Terlouw, B. R.; Tran, T. A.; Valentine, M.; van der Hooft, J. J. J.; Vo, D. A.; Wang, M.; Wilson, D.; Zink, K. E.; Linington, R. G. *ACS Cent. Sci.* **2019**, *5* (11), 1824−1833.

(8) Storme, J.-Y.; Golubic, S.; Wilmotte, A.; Kleinteich, J.; Velázquez, D.; Javaux, E. J. *Astrobiology* **2015**, *15* (10), 843−857.

(9) Morinaka, B. I.; Lakis, E.; Verest, M.; Helf, M. J.; Scalvenzi, T.; Vagstad, A. L.; Sims, J.; Sunagawa, S.; Gugger, M.; Piel, J. *Science* **2018**, *359* (6377), 779−782.

(10) Usvalampi, A. Microbial Production of Xylitol, L-Xylulose and L-Xylose. Doctoral thesis, School of Chemical Technology, 2013. http://urn.fi/URN:ISBN:978-952-60-5317-2.

(11) Brady, S. F.; Chao, C. J.; Clardy, J. *J. Am. Chem. Soc.* **2002**, *124* (34), 9968−9969.

(12) Jansen, R.; Kunze, B.; Reichenbach, H.; Höfle, G. *Eur. J. Org. Chem.* **2003**, *2003* (14), 2684−2689.

(13) Bhandari, S.; Bisht, K. S.; Merkler, D. J. *Front. Mol. Biosci.* **2022**, *8*, No. 801749.

(14) Brady, S. F.; Clardy, J. *J. Am. Chem. Soc.* **2000**, *122* (51), 12903−12904.

(15) Rachid, S.; Revermann, O.; Dauth, C.; Kazmaier, U.; Müller, R. *J. Biol. Chem.* **2010**, *285* (17), 12482−12489.
(16) Leão, P. N.; Martins, T. P.; Abt, K.; Reis, J. P. A.; Figueiredo, S.; Castelo-Branco, R.; Freitas, S. *Chem. Commun.* **2023**, *59* (30), 4436−4446.
(17) Gilchrist, C. L. M.; Booth, T. J.; Van Wersch, B.; Van Grieken, L.; Medema, M. H.; Chooi, Y.-H. *Bioinformatics Advances* **2021**, *1* (1), No. vbab016.
(18) Gilchrist, C. L. M.; Chooi, Y.-H. *Bioinformatics* **2021**, *37* (16), 2473−2475.
(19) Van Den Belt, M.; Gilchrist, C.; Booth, T. J.; Chooi, Y.-H.; Medema, M. H.; Alanjary, M. *BMC Bioinformatics* **2023**, *24* (1), 181.
(20) Navarro-Muñoz, J. C.; Selem-Mojica, N.; Mullowney, M. W.; Kautsar, S. A.; Tryon, J. H.; Parkinson, E. I.; De Los Santos, E. L. C.; Yeong, M.; Cruz-Morales, P.; Abubucker, S.; Roeters, A.; Lokhorst, W.; Fernandez-Guerra, A.; Cappelini, L. T. D.; Goering, A. W.; Thomson, R. J.; Metcalf, W. W.; Kelleher, N. L.; Barona-Gomez, F.; Medema, M. H. *Nat. Chem. Biol.* **2020**, *16* (1), 60−68.
(21) Reis, J. P. A.; Figueiredo, S. A. C.; Sousa, M. L.; Leão, P. N. *Nat. Commun.* **2020**, *11* (1), 1−9.

https://doi.org/10.1021/acs.jnatprod.4c00968
J. Nat. Prod. 2025, 88, 850−856